

## Materials and methods

Two antisense 9-mer oligonucleotides (AONs) and their target 9-mer RNA were chemically synthesized (Gene Design Inc., Japan); DNA9: d(XTCTTCTTX) (X = 5-methyl-dC), BNA<sup>NC</sup>9 gapmer with five DNA gaps: d(YZCTTCTZY) (Y = 5-methyl-C<sup>NC</sup>[N-Me], Z = T<sup>NC</sup>[N-Me]), RNA9: r(GAAGAAGAG). Previously, the DNA9/RNA9 hybrid duplex was successfully crystallized by Xiong and Sundaralingam.<sup>S1</sup> Therefore, we have chosen these sequences for the present structural studies. These oligonucleotides were purified by 20% polyacrylamide gel electrophoresis under a denaturing condition containing 3.2 M urea and then desalted by reversed-phase chromatography.

Stabilities of BNA<sup>NC</sup>9/RNA9 or DNA9/RNA9 duplexes were examined by UV melting temperature analyses. Sample solutions containing 2  $\mu$ M BNA<sup>NC</sup>9/RNA9 or DNA9/RNA9, 10 mM sodium cacodylate (pH 7.0) and 100 mM sodium chloride were prepared. The thermally induced transitions of these duplexes were monitored on a UV-VIS spectrophotometer (V630, JASCO corp., Japan). Relative absorbance,  $A = (A_t - A_{20^\circ\text{C}})/(A_{70^\circ\text{C}} - A_{20^\circ\text{C}})$ , at 260 nm versus temperature for the mixtures are shown in Fig. S1.

Formation abilities of BNA<sup>NC</sup>9/RNA9 and DNA9/RNA9 duplexes were examined by electrophoretic mobility shift assay. In a 20  $\mu$ L aliquot of the reaction mixture, RNA9 (5  $\mu$ M) was mixed with increasing concentrations of the complementary strand (BNA<sup>NC</sup>9 or DNA9) in buffer [10 mM Na cacodylate-cacodylic acid (pH 6.8) and 100 mM NaCl]. After 2 h incubation at 25  $^\circ\text{C}$ , 4  $\mu$ L of 4% sucrose solution containing bromophenol blue was added without changing the pH and salt concentrations of the reaction mixtures. Samples were then directly loaded onto a 15% native polyacrylamide gel prepared in buffer (89 mM Tris-borate), and electrophoresis was performed at 8 V/cm for 1.5 h at 25  $^\circ\text{C}$ . The gel was stained with SYBR Gold solution (Life Technologies) for 30 min at 25  $^\circ\text{C}$ . The obtained gel image is shown in Fig. S2.

Formation abilities of BNA<sup>NC</sup>10/RNA10 and DNA10/RNA10 duplexes (the same sequence as BNA<sup>NC</sup>9/RNA9 and DNA9/RNA9 duplex with an additional 3' single base overhang in both strands) were examined by BIACORE interaction analysis system using a BIACORE J instrument (GE Healthcare, U.S.A.), in which a real-time biomolecular interaction was measured with a laser biosensor. The layer of an SA sensor tip with immobilized streptavidin was equilibrated with 20 mM potassium phosphate buffer (pH 7.0) (buffer A) at a flow rate of 30  $\mu$ L/min. Biotinylated RNA10 (the same sequence as RNA9 with an additional G base at 3' end) (Bt-RNA10) solution in buffer A was added to bind with the streptavidin on the surface. 40  $\mu$ L of BNA<sup>NC</sup>10 or DNA10 (the same sequence as BNA<sup>NC</sup>9 or DNA9 with an additional C base at 3' end) solution in buffer A was injected over the immobilized Bt-RNA10 at a flow rate of 30  $\mu$ L/min, and then the duplex formation was monitored for 1 min. This was followed by washing the sensor tip with buffer A, and the dissociation of the preformed duplex was monitored for an additional 3 min. Finally, 130  $\mu$ L of 4 M urea solution for BNA<sup>NC</sup>10 or 40  $\mu$ L of 4 M urea solution for DNA10 was injected at a flow rate of 30  $\mu$ L/min to completely break the hydrogen bonding between Bt-RNA10 and the complementary strand (BNA<sup>NC</sup>10 or DNA10). The resulting sensorgrams were analyzed with the BIA evaluation software supplied by the manufacturer to calculate the kinetic parameters and the binding constants. The obtained sensorgrams and the calculated kinetic parameters and binding constants are shown in Fig. S3 and Table S1, respectively.

Crystallizations were performed at 20  $^\circ\text{C}$  by the hanging-drop vapour diffusion method by mixing 1  $\mu$ L of sample solution containing 1 mM BNA<sup>NC</sup>9/RNA9 or DNA9/RNA9 and 1  $\mu$ L of crystallization solution containing 50 mM sodium cacodylate (pH 7.0), 0-20 mM spermine tetrahydrochloride or hexamine cobalt chloride, 1-10% (v/v) 2-methyl-2,4-pentanediol and 10-750 mM cation chlorides, which was equilibrated against 250  $\mu$ L of 40% 2-methyl-2,4-pentanediol. Detailed crystallization conditions are summarized in Table S2.

X-ray datasets were collected at 100K with synchrotron radiation at the BL-17A and BL-5A beamlines of the Photon Factory (Tsukuba, Japan). For the phase determination with the multiple anomalous diffraction (MAD) method, the X-ray data of the BNA<sup>NC</sup>9/RNA9-Co and DNA9/RNA9-Co crystals were taken with three different wavelengths (1.60465, 1.60830 and 0.98 Å for the BNA<sup>NC</sup>9/RNA9-Co crystal, and 1.60366, 1.60546 and 1.0 Å for the DNA9/RNA9-Co crystal) based on XAFS measurements. X-Ray diffractions were recorded on CCD detectors (Quantum 315r and 210r). Diffraction patterns were taken using 2° oscillation with 1 s exposure per frame. Each dataset was processed with the program *CrystalClear* (Rigaku Americas Corp., The Woodlands, TX). Some statistics of data collections,  $R_{\text{meas}}$  and  $R_{\text{p.i.m.}}$ , were calculated with the program *merging\_statistics* from *Phenix* suite.<sup>S2-S4</sup> The intensity data obtained were further converted to structure-factor amplitudes using the program *TRUNCATE* from the *CCP4* suite.<sup>S5</sup> The statistics of data collections and the crystal data are summarized in Table S3.

The initial phases of the BNA<sup>NC</sup>9/RNA9-Co and DNA9/RNA9-Co crystals were estimated by the MAD method with the program *AutoSol* from *Phenix* suite<sup>S2, S6, S7</sup> with figure-of-merit of 0.72 and 0.44, respectively. By using the heavy-atom-search procedure of the program, three and one cobalt atoms were found in the asymmetric unit of the BNA<sup>NC</sup>9/RNA9-Co and DNA9/RNA9-Co crystals, respectively. The molecular structures of the BNA<sup>NC</sup>9/RNA9 and DNA9/RNA9 duplexes were constructed and manipulated with the programs *Coot*.<sup>S8, S9</sup> The coordinate and parameter files of 2',4'-BNA<sup>NC</sup>[N-Me]-modified residues, Y and Z, were constructed with *ChemOffice* (PerkinElmer Inc., Waltham, MA) and *HIC-Up* (*Hetero-compound Information Center - Uppsala*) server.<sup>S10</sup> The initial phase of the DNA9/RNA9-Sp was derived by the molecular replacement method with the program *AutoMR* from the *Phenix* suite.<sup>S2, S11</sup> For the molecular replacement, a refined crystal structure of DNA9/RNA9-Co was used as a model. The atomic parameters of each structure were refined using the program *CNS* through a combination of simulated-annealing, crystallographic conjugate gradient minimization refinements and *B*-factor refinements,<sup>S12, S13</sup> followed by interpretation of an omit map at every nucleotide residue. The statistics of structure refinements are summarized in Table S3. Molecular drawings shown in Fig. 2-4 and Fig. S4 were made using *PyMOL*.<sup>S14</sup> The local helical parameters and pseudorotation phase angles shown in Tables S4-S7 and Fig. S5 were calculated using the program *3DNA*.<sup>S15, S16</sup> The atomic coordinates and experimental data of BNA<sup>NC</sup>9/RNA9-Co, DNA9/RNA9-Co and DNA9/RNA9-Sp have been deposited in the Protein Data Bank (PDB) with the ID codes 4U6K, 4U6L and 4U6M, respectively.




## References

- S1. Y. Xiong, M. Sundaralingam, *Nucleic Acids Res.*, 2000, **28**, 2171-2176.
- S2. P. D. Adams, P. V. Afonine, G. Bunkóczi, V. B. Chen, I. W. Davis, N. Echols, J. J. Headd, L. W. Hung, G. J. Kapral, R. W. Grosse-Kunstleve, A. J. McCoy, N. W. Moriarty, R. Oeffner, R. J. Read, D. C. Richardson, J. S. Richardson, T. C. Terwilliger, P. H. Zwart, *Acta Crystallogr. D Biol. Crystallogr.*, 2010, **66**, 213-221.
- S3. K. Diederichs, P. A. Karplus, *Nat. Struct. Biol.*, 1997, **4**, 269-275.
- S4. M. S. Weiss, *J. Appl. Cryst.*, 2001, **34**, 130-135.
- S5. Collaborative Computational Project, Number 4. *Acta Crystallogr. D Biol. Crystallogr.*, 1994, **50**, 760-763.
- S6. R. W. Grosse-Kunstleve, P. D. Adams, *Acta Crystallogr. D Biol. Crystallogr.*, 2003, **59**, 1966-1973.
- S7. T. C. Terwilliger, P. D. Adams, R. J. Read, A. J. McCoy, N. W. Moriarty, R. W. Grosse-Kunstleve, P. V. Afonine, P. H. Zwart, L. W. Hung, *Acta Crystallogr. D Biol. Crystallogr.*, 2009, **65**, 582-601.
- S8. P. Emsley, K. Cowtan, *Acta Crystallogr. D Biol. Crystallogr.*, 2002, **60**, 2126-2162.
- S9. P. Emsley, B. Lohkamp, W. G. Scott, K. Cowtan, *Acta Crystallogr. D Biol. Crystallogr.*, 2010, **66**, 486-501.
- S10. G. J. Kleywegt, *Acta Crystallogr. D Biol. Crystallogr.*, 2007, **63**, 94-100.
- S11. A. J. McCoy, R. W. Grosse-Kunstleve, P. D. Adams, M. D. Winn, L. C. Storoni, R. J. Read, *J. Appl. Crystallogr.*, 2007, **40**, 658-674.
- S12. A. T. Brünger, P. D. Adams, G. M. Clore, W. L. DeLano, P. Gros, R. W. Grosse-Kunstleve, J. -S. Jiang, J. Kuszewski, M. Nilges, N. S. Pannu, R. J. Read, L. M. Rice, T. Simonson, G. L. Warren, *Acta Crystallogr. D Biol. Crystallogr.*, 1998, **54**, 905-921.
- S13. A. T. Brünger, *Nature*, 1992, **355**, 472-475.
- S14. W. L. DeLano, *The PyMOL Molecular Graphics System*. DeLano Scientific LLC, Palo Alto, CA, USA., 2008.
- S15. W. K. Olson, M. Banasal, S. K. Burley, R. E. Dickerson, M. Gerstein, S. C. Harvey, U. Heinemann, X. J. Lu, S. Neidle, Z. Shakked, H. Sklenar, M. Suzuki, C. -S. Tung, E. Westhof, C. Wolberger, H. Berman, *J. Mol. Biol.*, 2001, **313**, 229-237.
- S16. X. J. Lu, W. K. Olson, *Nucleic Acids Res.*, 2003, **31**, 5108-5121.

**Table S1.** Kinetic parameters and binding constants of the duplex formation between the target RNA (RNA10: the same sequence as RNA9 with an additional G base at 3' end) and the complementary strand (BNA<sup>NC</sup>10 or DNA10: the same sequence as BNA<sup>NC</sup>9 or DNA9 with an additional C base at 3' end) at 25 °C and pH 7.0 in 20 mM potassium phosphate buffer, obtained from BIACORE interaction analysis system

Complementary strand	$k_{\text{assoc}}$ ( $\text{M}^{-1} \text{s}^{-1}$ )	$k_{\text{dissoc}}$ ( $\text{s}^{-1}$ )	$K_{\text{a}}$ ( $\text{M}^{-1}$ )
BNA <sup>NC</sup> 10	$1.06 \times 10^4$	$3.91 \times 10^{-4}$	$2.71 \times 10^7$
DNA10	$2.09 \times 10^3$	$3.79 \times 10^{-2}$	$5.51 \times 10^4$

**Table S2.** Crystallization conditions

Crystal code	BNA <sup>NC</sup> 9/RNA9-Co	DNA9/RNA9-Co	DNA9/RNA9-Sp
Temperature	20 °C	20 °C	20 °C
<u>Sample solution (1 <math>\mu\text{l}</math>)</u>			
Antisense strand (BNA <sup>NC</sup> 9 or DNA9)	1 mM	1 mM	1 mM
Target RNA strand (RNA9)	1 mM	1 mM	1 mM
<u>Crystallization solution (1 <math>\mu\text{l}</math>)</u>			
Sodium cacodylate (pH = 7.0)	50 mM	50 mM	50 mM
Spermine tetrahydrochloride	-	-	10 mM
Hexamine cobalt chloride	10 mM	10 mM	-
Sodium chloride	100 mM	-	-
Potassium chloride	-	-	250 mM
Strontium chloride	100 mM	100 mM	-
2-Methyl-2,4-pentanediol	10%	10%	10%
<u>Reservoir solution (250 <math>\mu\text{l}</math>)</u>			
2-Methyl-2,4-pentanediol	40%	40%	40%
Crystals			
Size of crystal ( $\text{mm}^3$ )	$0.10 \times 0.05 \times 0.05$	$0.10 \times 0.07 \times 0.03$	$0.30 \times 0.07 \times 0.05$

**Table S3.** Crystal data, statistics of data collections and structure refinements

Crystal code	BNA <sup>NC</sup> 9/RNA9-Co		DNA9/RNA9-Co		DNA9/RNA9-Sp
PDB-ID	4U6K		4U6L		4U6M
Dataset	For MAD phasing <sup>h</sup>	For structure refinement <sup>i</sup>	For MAD phasing <sup>h</sup>	For structure refinement <sup>i</sup>	
<b>Crystal data</b>					
Space group	C222 <sub>1</sub>		P6 <sub>1</sub>		P6 <sub>1</sub>
Unit cell (Å)	<i>a</i> = 43.9, <i>b</i> = 59.0, <i>c</i> = 102.5		<i>a</i> = <i>b</i> = 48.5, <i>c</i> = 46.5		<i>a</i> = <i>b</i> = 49.1, <i>c</i> = 46.0
<i>Z</i> <sup>a</sup>	2		1		1
<b>Data collection</b>					
Beamline	BL-17A of PF		BL-5A of PF		BL-5A of PF
Wavelength (Å)	1.60465 / 1.60830 / 0.98		1.60366 / 1.60546 / 1.0		1.0
Resolution (Å)	51.2-1.6 / 51.2-1.6 / 25.6-1.5		24.3-2.0 / 24.3-2.0 / 42.0-1.9		42.0-1.9
of the outer shell (Å)	1.7-1.6 / 1.7-1.6 / 1.6-1.5		2.1-2.0 / 2.1-2.0 / 2.0-1.9		2.0-1.9
Unique reflections	32414 / 32465 / 40292		8252 / 8257 / 9653		4976
Completeness (%)	95.7 / 95.8 / 97.8		99.5 / 99.5 / 99.8		99.8
in the outer shell (%)	92.4 / 92.4 / 97.6		98.8 / 98.5 / 99.9		100.0
<i>R</i> <sub>merge</sub> <sup>b</sup> (%)	-		-		3.0
in the outer shell (%)	-		-		31.6
<i>R</i> <sub>anom</sub> <sup>c</sup> (%)	6.2 / 6.0 / 4.8		3.3 / 3.3 / 2.6		-
in the outer shell (%)	32.3 / 32.5 / 25.2		37.9 / 39.8 / 30.6		-
<i>R</i> <sub>meas</sub> <sup>d</sup> (%)	14.5 / 14.8 / 12.5		5.0 / 4.8 / 4.0		4.2
in the outer shell (%)	47.3 / 48.0 / 36.5		47.3 / 49.3 / 34.8		35.5
<i>R</i> <sub>p.i.m.</sub> <sup>e</sup> (%)	7.6 / 7.8 / 6.6		2.9 / 2.8 / 2.4		1.8
in the outer shell (%)	24.5 / 25.0 / 18.7		27.5 / 28.6 / 20.3 / 14.9		14.9
<i>I</i> / <i>σ</i> ( <i>I</i> )	9.4 / 9.4 / 13.6		19.7 / 19.8 / 25.8		32.6
in the outer shell	3.0 / 2.7 / 4.2		3.5 / 3.4 / 4.4		6.4
Redundancy	3.6 / 3.6 / 3.6		5.4 / 5.4 / 5.5		10.8
in the outer shell	3.6 / 3.6 / 3.6		5.3 / 5.3 / 5.5		10.8
<b>Structure refinement</b>					
Resolution range (Å)	25.6-1.5		42.0-1.9		42.5-1.9
Used reflections	21282		4975		5020
<i>R</i> -factor <sup>f</sup> (%)	19.8		25.1		20.7
<i>R</i> <sub>free</sub> <sup>g</sup> (%)	21.6		27.5		23.3
R.m.s.d. bond length (Å)	0.019		0.006		0.006
R.m.s.d. bond angles (°)	2.0		1.3		1.2

<sup>a</sup> Number of nucleotide duplex in the asymmetric unit.<sup>b</sup>  $R_{\text{merge}} = 100 \times \sum_{hkl} \sum_j |I_{hkl,j} - \langle I_{hkl} \rangle| / \sum_{hkl} \sum_j \langle I_{hkl} \rangle$ .<sup>c</sup>  $R_{\text{anom}} = 100 \times \sum_{hkl} \sum_j [I_{hkl,j}(+) - I_{hkl,j}(-)] / \sum_{hkl} \sum_j [I_{hkl,j}(+) + I_{hkl,j}(-)]$ .<sup>d</sup>  $R_{\text{meas}} = 100 \times \sum_{hkl} (N/(N-1))^{1/2} \sum_j |I_{hkl,j} - \langle I_{hkl} \rangle| / \sum_{hkl} \sum_j I_{hkl,j}$ <sup>e</sup>  $R_{\text{p.i.m.}} = 100 \times \sum_{hkl} (1/(N-1))^{1/2} \sum_j |I_{hkl,j} - \langle I_{hkl} \rangle| / \sum_{hkl} \sum_j I_{hkl,j}$ <sup>f</sup> R-factor =  $100 \times \sum ||F_o| - |F_c|| / \sum |F_o|$ , where  $|F_o|$  and  $|F_c|$  are optimally scaled observed and calculated structure factor amplitudes, respectively.<sup>g</sup> Calculated using a random set containing 10% of observations.<sup>h</sup> For phase determination with the multiple anomalous diffraction (MAD) method, three datasets were collected with three wavelengths. Statistics from left to right are of peak, edge and remote data, respectively.<sup>i</sup> For structure refinement, the remote dataset containing merged Friedel-pair reflections was used.

**Table S4.** Pseudorotation phase angles of sugar rings in the BNA<sup>NC</sup>9/RNA9 duplex. Values on left and right are of duplexes 1 and 2 observed in the BNA<sup>NC</sup>9/RNA9-Co crystal, respectively.

Nucleotides	Pseudorotation (°)	Puckering	Nucleotides*	Pseudorotation (°)	Puckering
<b>RNA9</b>			<b>BNA<sup>NC</sup>9</b>		
G <sub>1</sub>	4 / 2	C3'-endo	Y <sub>1</sub>	17 / 19	C3'-endo
A <sub>2</sub>	11 / 5	C3'-endo	Z <sub>2</sub>	18 / 17	C3'-endo
A <sub>3</sub>	8 / 11	C3'-endo	T <sub>3</sub>	15 / 17	C3'-endo
G <sub>4</sub>	9 / 14	C3'-endo	C <sub>4</sub>	15 / 16	C3'-endo
A <sub>5</sub>	6 / 8	C3'-endo	T <sub>5</sub>	16 / 15	C3'-endo
A <sub>6</sub>	13 / 11	C3'-endo	T <sub>6</sub>	22 / 16	C3'-endo
G <sub>7</sub>	14 / 14	C3'-endo	C <sub>7</sub>	17 / 17	C3'-endo
A <sub>8</sub>	9 / 9	C3'-endo	Z <sub>8</sub>	19 / 18	C3'-endo
G <sub>9</sub>	16 / 15	C3'-endo	Y <sub>9</sub>	21 / 20	C3'-endo
Average	10 / 10	C3'-endo	Average	18 / 17	C3'-endo
A-form	18	C3'-endo	A-form	18	C3'-endo
B-form	162	C2'-endo	B-form	162	C2'-endo

\*Y = 5-methyl-C<sup>NC</sup>[N-Me], Z = T<sup>NC</sup>[N-Me]

**Table S5.** Pseudorotation phase angles of sugar rings in the BNA9/RNA9 duplex. Values on left and right are of duplexes observed in the DNA9/RNA9-Co and DNA9/RNA9-Sp crystals, respectively.

Nucleotides	Pseudorotation (°)	Puckering	Nucleotides*	Pseudorotation (°)	Puckering
<b>RNA9</b>			<b>BNA9</b>		
G <sub>1</sub>	10 / 6	C3'-endo	X <sub>1</sub>	7 / 13	C3'-endo
A <sub>2</sub>	15 / 11	C3'-endo	T <sub>2</sub>	19 / 16	C3'-endo
A <sub>3</sub>	17 / 11	C3'-endo	T <sub>3</sub>	22 / 19	C3'-endo
G <sub>4</sub>	2 / 2	C3'-endo	C <sub>4</sub>	16 / 16	C3'-endo
A <sub>5</sub>	27 / 21	C3'-endo	T <sub>5</sub>	21 / 19	C3'-endo
A <sub>6</sub>	18 / 15	C3'-endo	T <sub>6</sub>	16 / 17	C3'-endo
G <sub>7</sub>	16 / 11	C3'-endo	C <sub>7</sub>	19 / 22	C3'-endo
A <sub>8</sub>	1 / 2	C3'-endo	T <sub>8</sub>	13 / 21	C3'-endo
G <sub>9</sub>	7 / 11	C3'-endo	X <sub>9</sub>	13 / 18	C3'-endo
Average	13 / 10	C3'-endo	Average	16 / 18	C3'-endo
A-form	18	C3'-endo	A-form	18	C3'-endo
B-form	162	C2'-endo	B-form	162	C2'-endo

\*X = 5-methyl-dC

**Table S6.** Local base pair helical parameters of the BNA<sup>NC</sup>9/RNA9 duplex. Values on left and right are of duplexes 1 and 2 observed in the BNA<sup>NC</sup>9/RNA9-Co crystal, respectively.

Base pair*	Inclination (°)	Tip (°)	Twist (°)	X-displacement (Å)	Y-displacement (Å)	Rise (Å)
G <sub>1</sub> =Y <sub>9</sub>						
A <sub>2</sub> -Z <sub>8</sub>	11 / 13	9 / 12	27 / 32	-5.4 / -5.1	-1.3 / 0.0	2.6 / 2.6
A <sub>3</sub> -T <sub>7</sub>	9 / 9	2 / 1	30 / 31	-4.3 / -3.9	0.9 / 0.6	2.9 / 3.0
G <sub>4</sub> =C <sub>6</sub>	2 / 10	2 / -1	26 / 28	-5.4 / -5.3	-0.5 / -0.8	3.4 / 3.0
A <sub>5</sub> -T <sub>5</sub>	10 / 14	-2 / -4	34 / 34	-4.3 / -4.7	1.8 / 1.3	3.0 / 2.9
A <sub>6</sub> -T <sub>4</sub>	12 / 12	0 / 2	34 / 30	-4.6 / -3.9	-0.7 / -0.6	3.0 / 2.8
G <sub>7</sub> =C <sub>3</sub>	8 / 8	-4 / -3	32 / 29	-6.2 / -4.8	-0.9 / -0.7	3.2 / 3.0
A <sub>8</sub> -Z <sub>2</sub>	17 / 11	2 / 0	26 / 34	-5.7 / -4.1	2.0 / 0.4	2.4 / 3.0
G <sub>9</sub> =Y <sub>1</sub>	15 / 5	6 / -4	25 / 29	-5.0 / -5.0	-0.6 / -0.3	2.4 / 3.0
Average	11 / 10	2 / 1	29 / 31	-5.0 / -4.6	-0.1 / 0.0	2.9 / 2.9
A-form <sup>#</sup>	15	0	33	-4.2	0.0	2.8
B-form <sup>#</sup>	2	0	37	0.1	0.0	3.3

\*Y = 5-methyl-C<sup>NC</sup>[N-Me], Z = T<sup>NC</sup>[N-Me]

<sup>#</sup> Values for the A- and B-form conformations are from reference S15.

**Table S7.** Local base pair helical parameters of the DNA9/RNA9 duplex. Values on left and right are of duplexes observed in the DNA9/RNA9-Co and DNA9/RNA9-Sp crystals, respectively.

Base pair*	Inclination (°)	Tip (°)	Twist (°)	X-displacement (Å)	Y-displacement (Å)	Rise (Å)
G <sub>1</sub> =X <sub>9</sub>						
A <sub>2</sub> -T <sub>8</sub>	5 / 3	-1 / -2	36 / 26	-2.1 / -2.2	-0.6 / -0.6	3.1 / 3.2
A <sub>3</sub> -T <sub>7</sub>	6 / 9	0 / 0	33 / 32	-2.5 / -3.1	-0.6 / -0.8	3.2 / 3.1
G <sub>4</sub> =C <sub>6</sub>	21 / 16	3 / 5	37 / 37	-3.7 / -3.6	1.8 / 1.7	2.9 / 3.0
A <sub>5</sub> -T <sub>5</sub>	28 / 26	-8 / -11	33 / 34	-5.7 / -5.4	-1.2 / -0.6	2.4 / 2.5
A <sub>6</sub> -T <sub>4</sub>	5 / 6	2 / 5	27 / 27	-3.4 / -3.8	-1.6 / -2.1	2.8 / 2.7
G <sub>7</sub> =C <sub>3</sub>	11 / 7	0 / -4	30 / 31	-4.5 / -4.0	-0.5 / 0.2	3.1 / 3.3
A <sub>8</sub> -T <sub>2</sub>	14 / 12	4 / 3	36 / 34	-3.8 / -3.4	0.9 / 1.2	2.9 / 2.9
G <sub>9</sub> =X <sub>1</sub>	4 / 4	-3 / -2	30 / 28	-4.0 / -4.3	-0.3 / -1.2	2.9 / 3.0
Average	12 / 10	0 / -1	33 / 33	-3.7 / -3.7	-0.3 / -0.3	2.9 / 3.0
A-form <sup>#</sup>	15	0	33	-4.2	0.0	2.8
B-form <sup>#</sup>	2	0	37	0.1	0.0	3.3

\*X = 5-methyl-dC

<sup>#</sup> Values for the A- and B-form conformations are from reference S15.

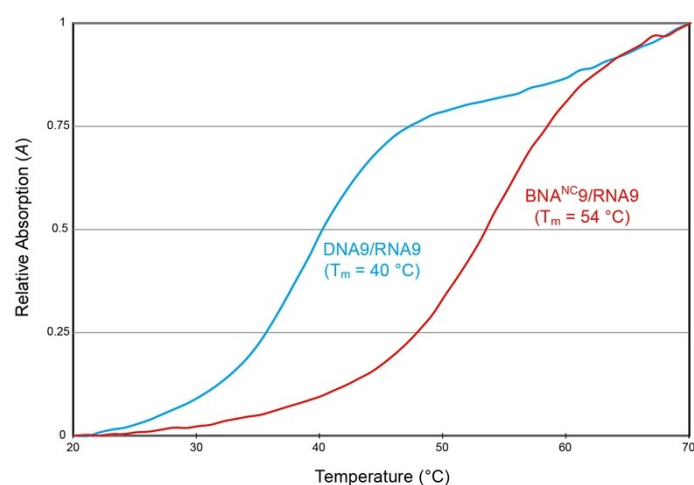


**Fig. S1.** Relative absorption,  $A = (A_{T\text{ }^{\circ}\text{C}} - A_{20\text{ }^{\circ}\text{C}})/(A_{70\text{ }^{\circ}\text{C}} - A_{20\text{ }^{\circ}\text{C}})$ , at 260 nm versus temperature for the BNA<sup>NC9</sup>/RNA9 (red) and DNA9/RNA9 (blue) duplexes.

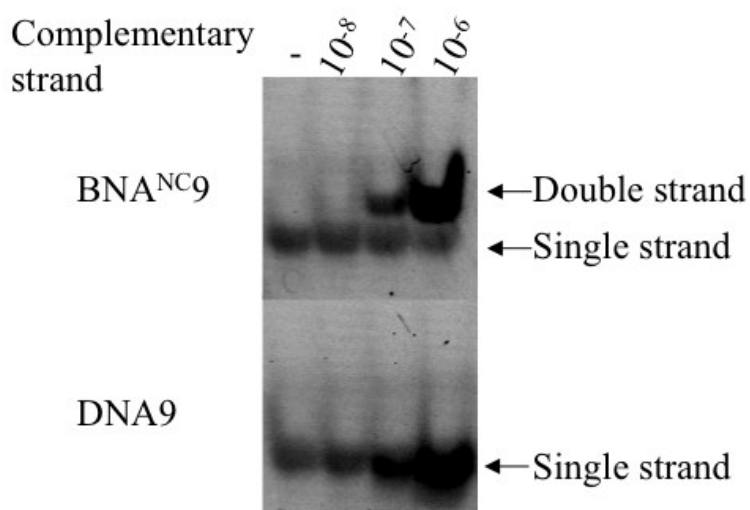


**Fig. S2.** Electrophoretic mobility shift assay of BNA<sup>NC9</sup>/RNA9 and DNA9/RNA9 duplex formation. Positions of double strand and single strand are indicated.



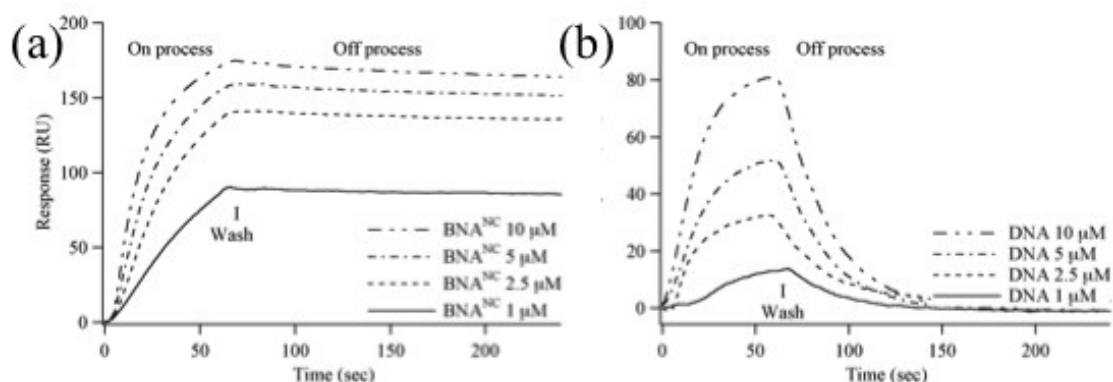


**Fig. S3.** BIAcore interaction analyses of BNA<sup>NC</sup>10/RNA10 (a) and DNA10/RNA10 (b) (the same sequence as BNA<sup>NC</sup>9/RNA9 and DNA9/RNA9 duplexes with an additional 3' single base overhang in both strands) duplex formation. The complementary strand (BNA<sup>NC</sup>10 or DNA10) solutions, diluted in the buffer to achieve the indicated final concentrations, were injected into the Bt-RNA10-immobilized cuvette. The binding of the complementary strand (BNA<sup>NC</sup>10 or DNA10) to Bt-RNA10 and the dissociation of the complementary strand (BNA<sup>NC</sup>10 or DNA10) from Bt-RNA10 were monitored as the response against time.

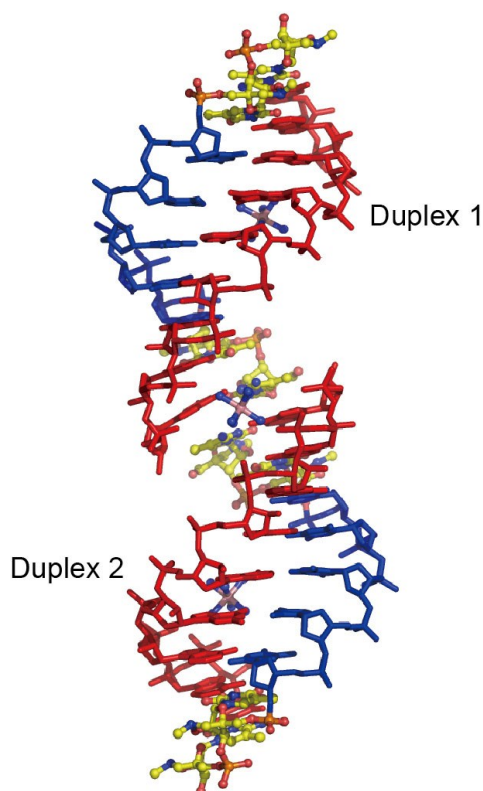


**Fig. S4.** Two duplexes observed in the asymmetric unit of the BNA<sup>NC</sup>9/RNA-Co crystal. Three

hexammine cobalt molecules are bound to the deep/major groove of these duplexes.

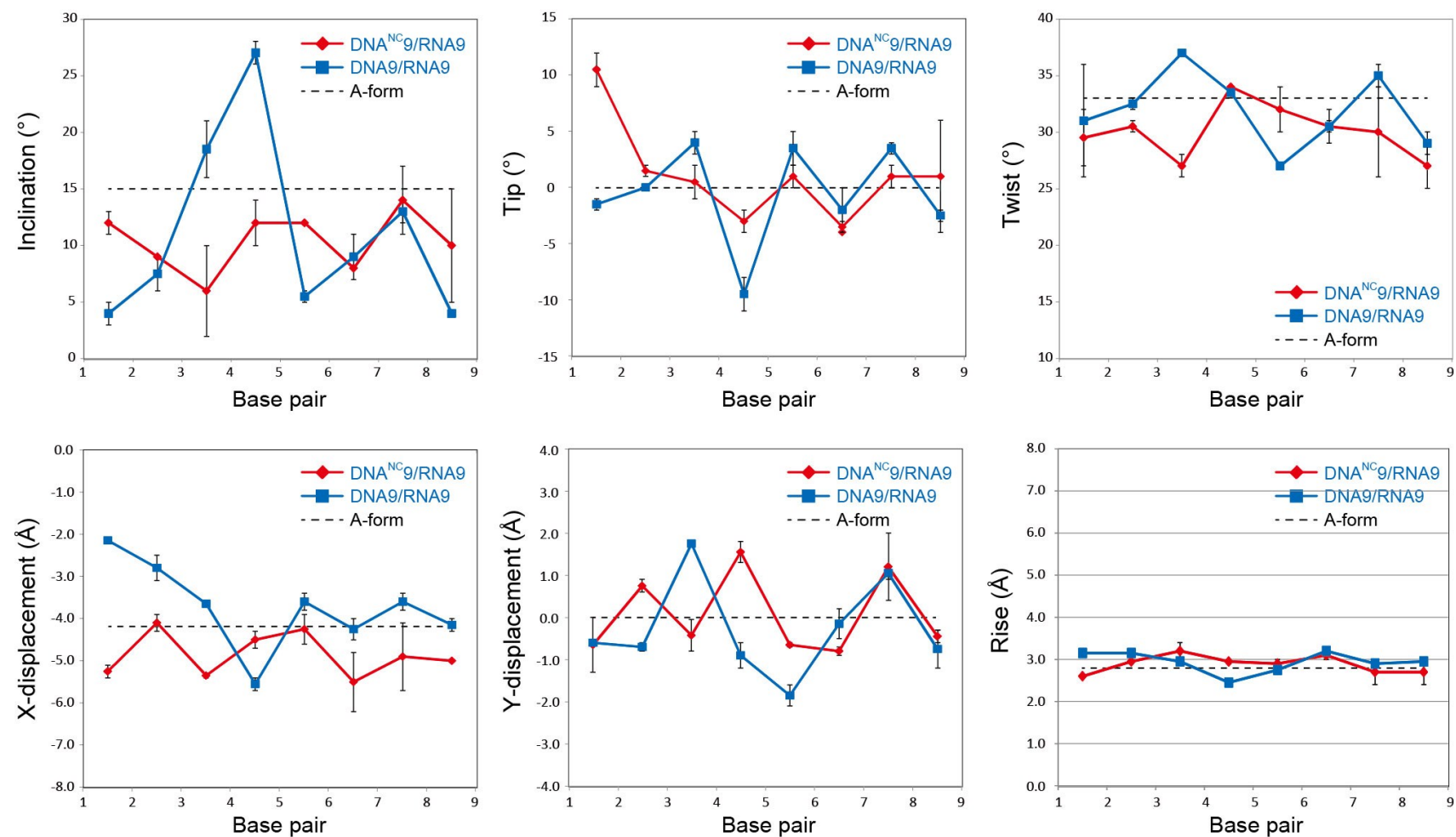


**Fig S5.** Local base pair helical parameters of the DNA<sup>NC</sup>9/RNA9 duplex (red: values for molecules 1 and 2 observed in the DNA<sup>NC</sup>9/RNA9-Co crystal are averaged) and the DNA9/RNA9 duplex (blue: values for duplexes observed in the DNA9/RNA9-Co and DNA9/RNA9-Sp crystals are averaged). Values for the A-form conformation (black dashed line) are from reference S11.